

## Crystal Structure and Magnetic Properties of $\text{Ba}_2\text{Ni}_3\text{F}_{10}$

M. LEBLANC, G. FERREY, AND R. DE PAPE

*Laboratoire des Fluorures et Oxyfluorures Ioniques, ERA 609, Faculté des Sciences, Route de Laval, 72017 Le Mans Cedex, France*

Received June 28, 1979

$\text{Ba}_2\text{Ni}_3\text{F}_{10}$  is monoclinic (space group  $C2/m$ ),  $a = 18.542(7)$  Å,  $b = 5.958(2)$  Å,  $c = 7.821(3)$  Å,  $\beta = 111^\circ 92'(10)$ .  $\text{Ba}_2\text{Co}_3\text{F}_{10}$  and  $\text{Ba}_2\text{Zn}_3\text{F}_{10}$  are isostructural. The structure has been refined from 995 reflections by full-matrix least-squares refinement to a weighted  $R$  value of 0.048 (unweighted  $R$ , 0.047). The three-dimensional network can be described either by complex chains connected to each other by octahedra sharing corners or with an 18L dense-packing sequence. The basic unit  $(\text{Ni}_3\text{F}_{10})^{4-}$  is discussed and compared to the different unit existing in  $\text{Cs}_4\text{Mg}_3\text{F}_{10}$ . Antiferromagnetic properties of  $\text{Ba}_2\text{Ni}_3\text{F}_{10}$  ( $T_N = 50$  K) are described.

### Introduction

The binary systems  $\text{AF}_2\text{-MF}_2$ , in which  $A$  is Ca, Sr, Ba and  $M$  is a  $3d$  transition metal, have been extensively studied during the last 20 years, particularly for a  $M/A$  ratio  $\leq 1$  (1-18). Two types of compounds are found in this domain:  $\text{AMF}_4$  with scheelite (3), difluorine (10), or  $\text{BaZnF}_4$  structures (6, 17) and  $\text{A}_2\text{MF}_6$  (5, 18). All these compounds, except Zn compounds, are two-dimensional magnets.

On the contrary, in these systems, only a few compounds with  $M/A > 1$  appear, and only when  $A = \text{Ba}$ . They are  $\text{Ba}_5\text{M}_6\text{F}_{22}$  ( $M = \text{Cu, Zn}$ ) (14, 15),  $\text{Ba}_2\text{M}_3\text{F}_{10}$  ( $M = \text{Zn}$ ) (5),  $\text{Co, Ni}$  (16)), and  $\text{Ba}_2\text{M}_7\text{F}_{18}$  ( $M = \text{Ni, Cu, Zn}$ ) (16)). Their structures have been unknown. From their composition, near that of rutile, it can be expected that with paramagnetic  $M^{2+}$  ions, a tight association of  $\text{MF}_6$  octahedra will occur, thus giving strong magnetic interactions, particularly with  $\text{Ni}^{2+}$ . This magnetic interest for the

phases led us to solve first the crystal structure of  $\text{Ba}_2\text{Ni}_3\text{F}_{10}$ .

### Experimental

$\text{Ba}_2\text{Ni}_3\text{F}_{10}$  single crystals were obtained by long heating at  $950^\circ\text{C}$  of the required quantities of  $\text{BaF}_2$  and  $\text{NiF}_2$  in a sealed platinum tube. As previously described (4, 16) powder diffraction patterns showed them to be monoclinic. The subsequent experimental data are listed in Table I.

The intensity data were collected on a CAD 4 Nonius diffractometer,<sup>1</sup> using  $\text{MoK}\alpha$  radiation in the range  $0 \leq h \leq 26$ ,  $-8 \leq k \leq 8$ ,  $-10 \leq l \leq 10$  with restrictive conditions corresponding to a  $C$  lattice. Operating features were previously described (23). The absorption correction was then applied using the numerical Gauss method in the AGNOST B program (25)

<sup>1</sup> Inorganic Crystallochemistry Laboratory (Professor Hardy), Faculty of Sciences, Poitiers, France.

TABLE I  
EXPERIMENTAL DATA FOR Ba<sub>2</sub>Ni<sub>3</sub>F<sub>10</sub> CRYSTALS

Symmetry:	Monoclinic
Space group:	C2/m
Conditions:	$h + k = 2n$
$\rho_{\text{exp}}$ :	$5.29 \pm 0.03$
$\rho_{\text{calc}}$ :	5.317
Cell parameters:	
$a$	$18.542 (7) \text{ \AA}$
$b$	$5.958 (2) \text{ \AA}$
$c$	$7.821 (3) \text{ \AA}$
$\beta$	$111.92 (10)$
$z$	4
Crystal dimension:	$(0.106 \times 0.078 \times 0.050) \text{ mm}^3$
$\mu \text{ MoK}\alpha$ :	$166 \text{ cm}^{-1}$

with  $\mu = 166 \text{ cm}^{-1}$ . After averaging, 995 independent reflections were used for the refinement of the structure.

### Structure Determination

The structure has been solved using the centrosymmetric space group C2/m. Refinements in noncentrosymmetric C2 and Cm groups do not give any significant improvement of the results. A tridimensional Patterson map was calculated using the MAXE program (26). Refinement by

full-matrix least-squares calculations was realized using a modified SFLS-5 program (27). The minimized function is  $\sum \omega (|F_o| - Z_k |F_c|)^2$  where  $F_o$  and  $F_c$  are observed and calculated structure factors,  $Z_k$  is a scale factor defined by  $Z_k = \sum |F_o| / \sum |F_c|$ , and  $\omega$  is the weighting. The Ibers weighting scheme, described in its final form by Grant *et al.* (28), has been used with  $p = 0.04$  for  $1/\omega = \sigma^2(F_o) = K\sigma(I)^2/4LpI + p^2I$ . Scattering factors for barium, nickel, and fluorine were calculated using Vand's relation (29–31). The anomalous dispersion corrections  $\Delta f'$  and  $\Delta f''$  are taken from the International Tables for X-Ray Crystallography (32).

The analysis of the Patterson map leads to localization of barium atoms in 4i sites. After refinement of the positional parameters of these atoms to an R value of 0.442, a Fourier map allows us to fix Ni(2) and Ni(3) in 4i and 4h sites. The residual falls to 0.297 after the refinement of their atomic coordinates. Ni(1) and all the fluorine atoms were then localized using a difference Fourier map. The adjustment of positional and isotropic thermal parameters of all atoms leads to  $R = 0.073$  ( $\omega R = 0.075$ ) using in the last two cycles of secondary extinction factor of  $0.414 \times 10^{-4}$ . With anisotropic temperature

TABLE II  
FINAL ATOMIC COORDINATES AND ANISOTROPIC TEMPERATURE FACTORS IN Ba<sub>2</sub>Ni<sub>3</sub>F<sub>10</sub><sup>a,b</sup>

Atom	Site	x	y	z	$U_{11} \cdot 10^4$	$U_{22} \cdot 10^4$	$U_{33} \cdot 10^4$	$U_{23} \cdot 10^4$	$U_{13} \cdot 10^4$	$U_{12} \cdot 10^4$	Beq.
Ba1	4i	0.1140(1)	0	0.2206(1)	78(4)	36(4)	80(4)	0	21(3)	0	0.45(2)
Ba2	4i	0.2165(1)	0	0.8141(1)	87(4)	42(4)	77(4)	0	21(3)	0	0.49(2)
Ni1	4i	0.4252(1)	0	0.0397(2)	61(6)	20(7)	56(7)	0	2(5)	0	0.38(3)
Ni2	4i	0.3221(1)	0	0.4829(2)	56(7)	12(7)	57(7)	0	10(5)	0	0.40(3)
Ni3	4h	0	0.7527(3)	1/2	64(6)	17(7)	68(7)	0	16(5)	0	0.38(3)
F1	8j	0.1114(3)	0.2421(9)	0.5263(7)	73(23)	41(25)	120(23)	8(19)	26(18)	5(20)	0.66(9)
F2	8j	0.3505(4)	0.2379(9)	0.0257(8)	175(23)	67(25)	116(23)	37(19)	94(19)	86(22)	0.99(9)
F3	4i	0.4783(5)	0	0.3157(10)	134(36)	34(33)	72(33)	0	50(28)	0	0.76(13)
F4	4i	0.3667(5)	0	0.7549(10)	99(34)	251(48)	58(35)	0	-6(29)	0	1.05(14)
F5	4i	0.0185(4)	0	0.6829(10)	111(36)	74(35)	74(33)	0	48(28)	0	1.14(15)
F6	4i	0.2633(6)	0	0.2177(12)	159(40)	267(50)	90(35)	0	41(30)	0	1.67(17)
F7	4g	0	0.2770(13)	0	116(32)	9(31)	113(34)	0	37(26)	0	0.67(12)
F8	4e	1/4	1/4	1/2	127(35)	76(39)	266(44)	-17(32)	84(31)	36(32)	1.37(16)

<sup>a</sup> Estimated standard deviations are given in parentheses.

<sup>b</sup> The vibrational coefficients relate to the expression:  $T = \exp[-2\pi^2(U_{11}h^2a^{*2} + U_{22}k^2b^{*2} + U_{33}l^2c^{*2} + 2U_{12}hka^{*}b^{*} + 2U_{13}kla^{*}c^{*} + 2U_{23}klb^{*}c^{*})]$ .

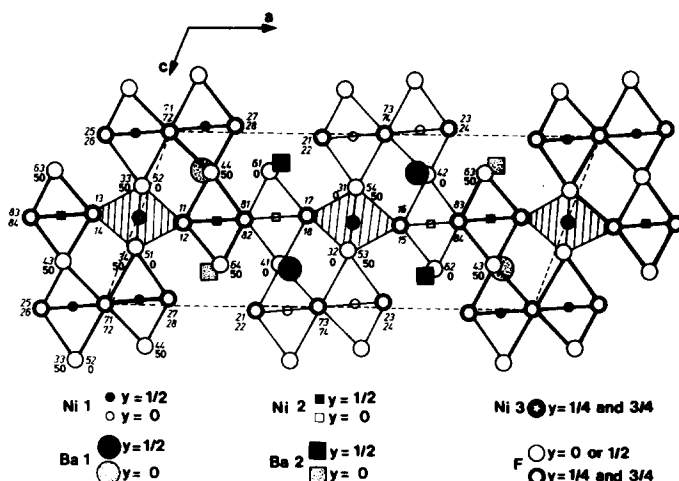


FIG. 1. (010) projection of  $\text{Ba}_2\text{Ni}_3\text{F}_{10}$ . For fluorine atoms, italic numbers correspond to the type and Wyckoff positions of atoms (see Table III); roman numbers indicate  $y$  coordinates of  $\text{F}^-$ .

factors, the residual becomes  $R = 0.048$  ( $\omega R = 0.047$ )<sup>2</sup> without any reject. Table II presents the final results for the 13 independent positions.

### Discussion of the Structure

Figure 1 presents the (010) projection of the three-dimensional network of  $\text{Ba}_2\text{Ni}_3\text{F}_{10}$ . Nickel atoms occupy three types of crystallographic sites. In the (002) plane, octahedra of Ni(3) atoms form infinite rutile chains parallel to the  $b$  axis of the cell, the dimension of which corresponds to two edge-sharing octahedra. Two complex satellites of three octahedra are connected to the rutile chains as represented in Fig. 2. Each satellite is "L" shaped, the central octahedron sharing, respectively, a vertex and the opposite edge of the same face with the two other octahe-

dra. These complex chains are linked together by the vertex of the satellites in order with respect to the  $C$  lattice of the cell (Fig. 3).

If the octahedra of Ni(3) are quite regular (Figs. 4a, b, and c), those of Ni(2) and Ni(1) exhibit, respectively, a slight angular distortion and a rather large distribution of distances (Table III); nevertheless, the average value of Ni–F distances, 2.007 Å, is close to the sum of ionic radii of hexacoordinated  $\text{Ni}^{2+}$  (0.69 Å) and tricoordinated  $\text{F}^-$  (1.30 Å) (19).

The coordination polyhedra of Ba(1) and Ba(2) can be easily described if the (20 $\bar{1}$ )

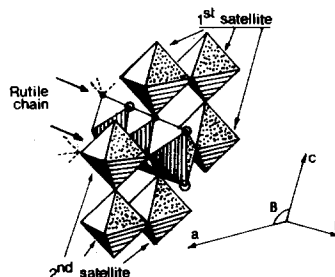


FIG. 2. Perspective view of the connection of the two satellites to a rutile chain. Solid circles are relative to the fluorines of the rutile chain which are shared to the satellite. Open circles are free.

<sup>2</sup> See NAPS document No. 03647 for 5 pages of supplementary material. Order from NAPS c/o Microfiche Publications, P.O. Box 3513, Grand Central Station, New York, N.Y. 10017. Remit in advance, in U.S. funds only \$5.00 for photocopies or \$3.00 for microfiche. Outside the U.S. and Canada add postage of \$3.00 for photocopy and \$1.00 for microfiche.

TABLE III  
INTERATOMIC DISTANCES, POLYHEDRAL EDGE LENGTHS, AND  
BOND ANGLES<sup>a</sup>

Octahedron of Ni(1) [0.0772; 1/2; 0.9603]: Symmetry <i>m</i>	
2 × Ni-F27 1.935(2) Å	1 × F27-F28 = 2.861(4) Å
1 × Ni-F34 2.006(2)	2 × F28-F34 2.959(4)
1 × Ni-F44 2.067(2)	2 × F28-F44 2.654(4)
2 × Ni-F71 2.069(2)	2 × F28-F72 2.854(4)
	1 × F73-F34 2.957(5)
	2 × F73-F41 2.837(4)
	2 × F73-F74 2.687(4)
$\bar{d}_{\text{Ni-F}} = 2.014 \text{ \AA}$	
1 × F28-Ni(1)-F27 95°33(11)	1 × F73-Ni(1)-F34 93°06(11)
2 × F28-Ni(1)-F34 97°31(11)	2 × F73-Ni(1)-F41 86°61(10)
2 × F28-Ni(1)-F44 82°89(10)	2 × F73-Ni(1)-F74 80°97(10)
2 × F28-Ni(1)-F72 90°86(10)	
Octahedron of Ni(2) [0.1780; 1/2; 0.5174]: Symmetry <i>m</i>	
2 × Ni(2)-F11 1.989(2) Å	2 × F11-F81 2.653(4) Å
1 × Ni(2)-F44 1.986(2)	1 × F11-F12 3.075(4)
1 × Ni(2)-F64 1.958(2)	2 × F11-F44 2.850(4)
2 × Ni(2)-F81 2.038(2)	2 × F11-F64 2.883(4)
	1 × F81-F82 2.979(5)
$\bar{d}_{\text{Ni-F}} = 2.000 \text{ \AA}$	2 × F81-F44 2.769(4)
	2 × F81-F64 2.758(4)
2 × F11-Ni(2)-F81 82°41(9)	1 × F81-Ni(2)-F82 93°92(11)
1 × F11-Ni(2)-F12 101°24(11)	2 × F81-Ni(2)-F44 86°93(9)
2 × F11-Ni(2)-F44 91°58(10)	2 × F81-Ni(2)-F64 87°26(9)
2 × F11-Ni(2)-F64 93°82(11)	
Octahedron of Ni(3) [0; 0.7529; 1/2]: Symmetry 2	
2 × Ni(3)-F12 2.000(2) Å	2 × F12-F51 2.852(4) Å
2 × Ni(3)-F51 1.995(2)	2 × F12-F52 2.765(4)
2 × Ni(3)-F33 2.026(2)	2 × F12-F33 2.858(4)
	2 × F12-F34 2.868(4)
	1 × F33-F34 2.709(4)
$\bar{d}_{\text{Ni-F}} = 2.007 \text{ \AA}$	2 × F33-F52 2.980(5)
	1 × F51-F52 2.692(4)
F12-Ni(3)-F51 91°11(10)	F33-Ni(3)-F34 83°90(9)
F12-Ni(3)-F52 87°58(9)	F33-Ni(3)-F52 95°64(11)
F12-Ni(3)-F33 90°46(10)	F51-Ni(3)-F52 84°87(9)
F12-Ni(3)-F34 90°86(10)	

<sup>a</sup> Fluorine atoms are noted by two numbers: the first refers to the type of fluorine noted in Table II, the second characterizes the coordinates of equivalent positions of a given Wyckoff position in the order of International Tables, for example;

F2(8j)	21. <i>xyz</i>	22. <i>x̄yz</i>
	23. <i>x̄ȳz̄</i>	24. <i>x̄ȳz̄</i>
	25. $1/2 + x, 1/2 + y, z$	26. $1/2 + x, 1/2 - y, z$
	27. $1/2 - x, 1/2 + y, \bar{z}$	28. $1/2 - x, 1/2 - y, \bar{z}$

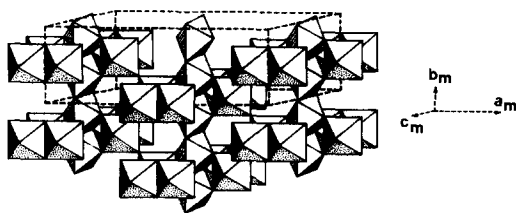


FIG. 3. Perspective view of Ba<sub>2</sub>Ni<sub>3</sub>F<sub>10</sub> structure.

planes of the structure are considered: barium and fluoride ions form together slightly distorted dense-packing layers parallel to these planes; barium ions thus adopt the 12 coordination characteristic of this type of packing. In the pseudoorthorhombic cell (Fig. 5) obtained by the matrix

$$\begin{bmatrix} a_0 \\ b_0 \\ c_0 \end{bmatrix} = \begin{bmatrix} 1 & 0 & 4 \\ 0 & 1 & 0 \\ 1 & 0 & 2 \end{bmatrix} \begin{bmatrix} a_m \\ b_m \\ c_m \end{bmatrix}$$

the structure can be described in terms of the dense packing with 18 layers (18L) corresponding to the sequence A<sub>1</sub>B<sub>2</sub><sup>2</sup>A<sub>2</sub><sup>2</sup>B<sub>1</sub><sup>2</sup>C<sub>2</sub><sup>2</sup> B<sub>2</sub><sup>2</sup>C<sub>4</sub><sup>2</sup>A<sub>2</sub><sup>2</sup>C<sub>2</sub><sup>2</sup>A<sub>4</sub><sup>2</sup>B<sub>2</sub><sup>2</sup>A<sub>2</sub><sup>2</sup>B<sub>1</sub><sup>2</sup>C<sub>2</sub><sup>2</sup>B<sub>2</sub><sup>2</sup>C<sub>4</sub><sup>2</sup>A<sub>2</sub><sup>2</sup>C<sub>2</sub><sup>2</sup>A<sub>1</sub><sup>2</sup> (the upper indices refer to the type of Ba which is inserted in the considered layer and the

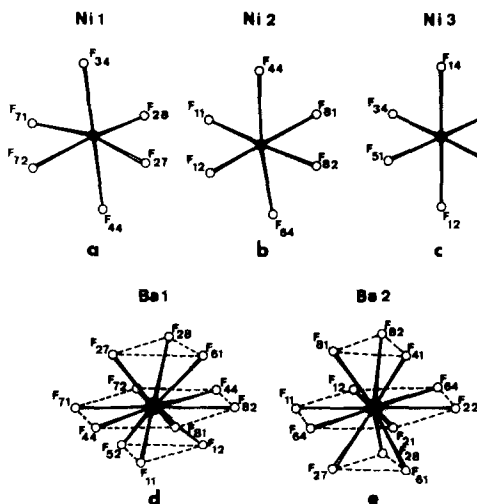


FIG. 4. Coordination polyhedra of Ni(1), Ni(2), Ni(3), Ba(1), and Ba(2). Symbols for fluorine atoms refer to Table III. They correspond to the (010) projection of Fig. 1.

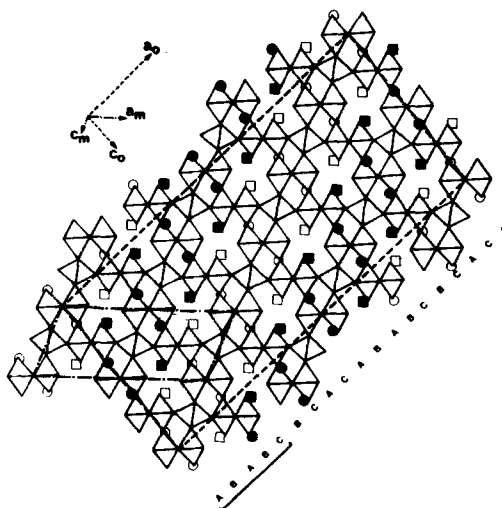


FIG. 5. Representation of Ba<sub>2</sub>Ni<sub>3</sub>F<sub>10</sub> in terms of 18L dense packing. Ba<sup>2+</sup> ions are represented in the same way as in Fig. 1.

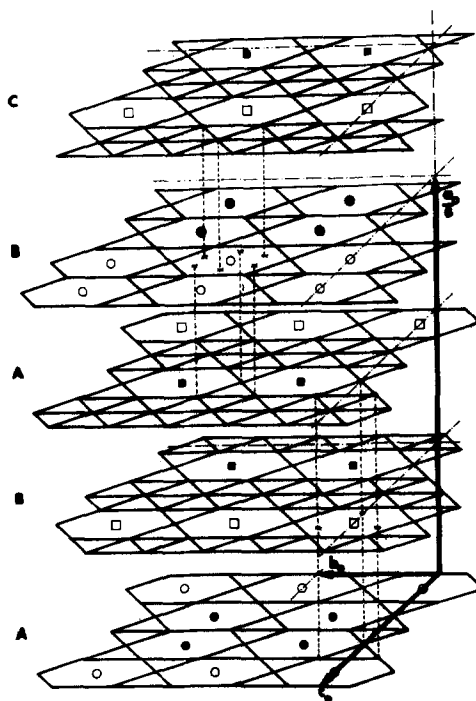


FIG. 6. Perspective view of the five layers ABABC, noted by a bracket in Fig. 5. It shows the two types of surroundings of Ba<sup>2+</sup> (the symbols are explained in Fig. 1). Fluoride ions occupy the intersection of the lines in each plane.

lower indices to the number of barium ions in the layer  $\text{Ba}_2\text{F}_{14}$  or  $\text{Ba}_4\text{F}_{12}$ ). This packing is twice the 9R packing occurring in  $\text{CsCoF}_3$  (21), the  $y$  coordinate of Ni and Ba atoms requiring doubling of the  $a$  and  $c$  parameters of a  $\text{CsCoF}_3$  pseudocell. It can be seen that barium adopts both the 12 coordination existing in *fcc* for Ba(1) and that existing in *hcp* for Ba(2) (Figs. 4d and e and Fig. 6). In both cases (Table IV), the average value of the Ba-F distances (2.851 and 2.878 Å) is close to the sum of ionic radii ( $r_{\text{Ba}^{2+}} = 1.61$  Å), but the F-F distance is always greater than  $2r_{\text{F}^-} = 2.60$  Å. It can be thought that the insertion of  $\text{Ba}^{2+}$  ions in the fluorine layers is responsible for this observed increasing of distance between  $\text{F}^-$  ions, and consequently for the lowering of the packing ratio from the ideal value of 0.74 to 0.65.

$\text{Ba}_2\text{Zn}_3\text{F}_{10}$  (4) and  $\text{Ba}_2\text{Co}_3\text{F}_{10}$  (16) are isotypic to  $\text{Ba}_2\text{Ni}_3\text{F}_{10}$ . Their  $b$  parameter, determined by two octahedra of the rutile chains of the structure, is always lower

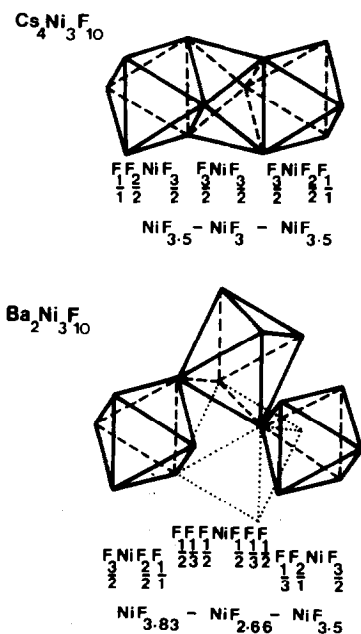


FIG. 7. Comparison of the  $(\text{Ni}_3\text{F}_{10})^{4-}$  groups existing in  $\text{Cs}_4\text{Ni}_3\text{F}_{10}$  and  $\text{Ba}_2\text{Ni}_3\text{F}_{10}$ .

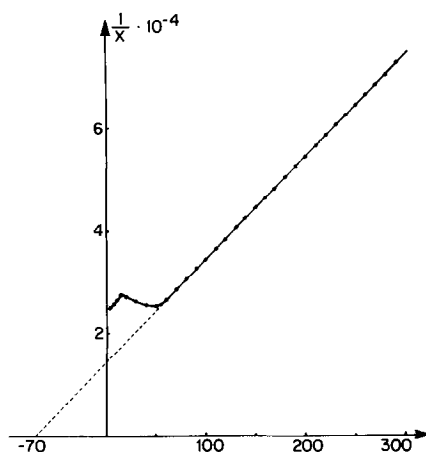


FIG. 8. Thermal variation of the inverse susceptibility of  $\text{Ba}_2\text{Ni}_3\text{F}_{10}$ .

than twice the  $c$  parameter of the corresponding rutile compounds  $\text{ZnF}_2$  and  $\text{CoF}_2$ .

In  $\text{Ba}_2\text{Ni}_3\text{F}_{10}$  appears a new structural group  $(\text{Ni}_3\text{F}_{10})^{4-}$  (Fig. 7). The same formula group exists in  $\text{Cs}_4\text{Ni}_3\text{F}_{10}$ , synthesized by Babel (20), but without any structural resemblance (22) to the group presently described. In  $\text{Cs}_4\text{Ni}_3\text{F}_{10}$ , the basic unit consists of three octahedra in which the central octahedron shares two opposing faces with the other two octahedra; on these, two of the three remaining vertices are connected to other basic units.

### Magnetic Properties

Magnetic measurements were realized from 4.2 to 300 K using a vibrating sample magnetometer.  $M(H)$  curves are strictly linear at every temperature. The inverse susceptibility (Fig. 8) is characteristic of antiferromagnetic behavior, and minimizes as  $T_N = 50$  K. Above 70 K, it obeys a Curie-Weiss law, which leads to  $\theta_p = -70$  K, and a molar Curie constant of  $3.03 \pm 0.05$  ( $C_M \text{ th.} = 3$ ). The relatively low value of  $\theta_p$  may be explained by competition between ferromagnetic Ni-Ni  $90^\circ$  exchange interactions existing in rutile-like blocks

TABLE IV  
INTERATOMIC DISTANCES, POLYHEDRAL EDGE LENGTHS, AND BOND ANGLES

Surrounding of Ba(1) [0.1140; 0; 0.2205]: Symmetry <i>m</i>		
2 × Ba(1)–F11 2.813(4) Å	1 × F11–F12 2.883(4) Å	2 × F52–F11 2.765(4) Å
2 × Ba(1)–F27 2.737(4)	2 × F11–F81 2.653(4)	1 × F71–F72 3.272(5)
2 × Ba(1)–F44 2.999(5)	1 × F27–F28 3.098(5)	2 × F71–F27 2.854(4)
2 × Ba(1)–F71 2.719(4)	2 × F27–F61 2.729(4)	2 × F71–F52 3.090(5)
2 × Ba(1)–F81 3.040(5)	2 × F44'–F28 2.654(4)	2 × F71–F44 2.837(4)
1 × Ba(1)–F52 2.823(4)	2 × F44'–F12 2.850(4)	1 × F81–F82 2.979(4)
1 × Ba(1)–F61 2.778(4)	2 × F44'–F82 2.769(4)	2 × F81–F61 2.758(4)
$\bar{d}_{\text{Ba-F}} = 2.851 \text{ \AA}$		$\bar{d}_{\text{F-F}} = 2.840 \text{ \AA}$
1 × F71–Ba(1)–F72 73°97'(16)		1 × F27–Ba(1)–F28 68°92'(13)
2 × F71–Ba(1)–F44 59°25'(9)		2 × F27–Ba(1)–F61 59°32'(9)
2 × F44'–Ba(1)–F82 54°57'(9)		1 × F11–Ba(1)–F12 61°66'(10)
1 × F81–Ba(1)–F82 58°67'(10)		2 × F11–Ba(1)–F52 58°76'(10)
2 × F44'–Ba(1)–F28 54°89'(9)		2 × F44'–Ba(1)–F12 58°65'(10)
2 × F71–Ba(1)–F27 63°07'(12)		2 × F71–Ba(1)–F52 67°75'(13)
2 × F81–Ba(1)–F61 56°37'(10)		2 × F82–Ba(1)–F12 53°74'(9)
1 × F44–Ba(1)–F44' 166°94'(21)		2 × F71–Ba(1)–F82 172°07'(20)
1 × F61–Ba(1)–F52 166°36'(18)		2 × F12–Ba(1)–F27 167°10'(9)
Surrounding of Ba(2) [0.2164; 0; 0.814]: Symmetry <i>m</i>		
2 × Ba(2)–F11 2.763(4) Å		1 × F11–F12 2.883(4) Å
		2 × F11–F64 2.883(4)
		1 × F21–F22 2.861(4)
2 × Ba(2)–F21 2.812(4)		2 × F21–F64 2.729(4)
		1 × F81–F82 2.979(5)
2 × Ba(2)–F64 3.024(5)		2 × F81–F41 2.769(4)
		2 × F81–F64 2.758(4)
1 × Ba(2)–F41 2.980(5)		2 × F81–F11 2.653(4)
2 × Ba(2)–F81 3.128(5)		2 × F21–F41 2.654(4)
		2 × F27–F11 3.300(6)
1 × Ba(2)–F61 2.934(5)		2 × F27–F64 2.949(5)
2 × Ba(2)–F27 2.582(4)		1 × F27–F28 3.098(5)
		2 × F27–F61 2.729(4)
		2 × F21–F61 2.949(5)
$\bar{d}_{\text{Ba-F}} = 2.878 \text{ \AA}$		$\bar{d}_{\text{F-F}} = 2.862 \text{ \AA}$
Angles		
1 × F11–Ba(2)–F12 62°90'(10)		2 × F11–Ba(2)–F81 53°10'(8)
2 × F11–Ba(2)–F64 59°55'(9)		2 × F64–Ba(2)–F81 53°23'(8)
1 × F21–Ba(2)–F22 61°16'(10)		2 × F21–Ba(2)–F41 54°44'(8)
2 × F21–Ba(2)–F64 55°62'(8)		
1 × F81–Ba(2)–F82 56°88'(9)		2 × F11–Ba(2)–F27 76°18'(11)
2 × F41–Ba(2)–F81 53°84'(8)		2 × F64–Ba(2)–F27 62°89'(10)
1 × F27–Ba(2)–F28 73°73'(10)		2 × F21–Ba(2)–F61 61°71'(10)
2 × F27–Ba(2)–F61 58°90'(9)		
1 × F64–Ba(2)–F64' 160°26'(18)		F11–Ba(2)–F22 160°63'(18)

and antiferromagnetic exchange interactions occurring when octahedra share only corners. Further neutron diffraction study will determine these different interactions.

## Conclusion

This study has shown the structural originality of products in which  $M/\text{Ba} > 1$ . This

first structure allows one to think that there would exist modulated structures between  $AMF_4$  and rutile. In this context, the study of  $Ba_2NiCrF_9$  (24), the parameters of which are close to those of  $Ba_2Ni_3F_{10}$ , and of  $Ba_2Ni_7F_{18}$  has begun.

### Acknowledgments

The authors are grateful to Drs. Samouel and de Kozak for useful chemical discussions, to Professor A. Hardy and Dr. A. M. Hardy for providing us facilities for data collection, and to Drs. Coey, Massenet, Dang, and Buder for their kind hospitality during magnetic measurements at the Groupe des Transitions de Phases (CNRS, Grenoble).

### References

1. E. INGERSON AND G. W. MOREY, *Amer. Mineral.* **36**, 778 (1951).
2. R. HOPPE, *Rec. Trav. Chim. Pays-Bas* **75**, 569 (1956).
3. H. G. VON SCHNERING AND P. BLECKMAN, *Naturwissenschaften* **52**, 538 (1965).
4. H. G. VON SCHNERING, *Z. Anorg. Allg. Chem.* **353**, 1 (1967).
5. H. G. VON SCHNERING, *Z. Anorg. Allg. Chem.* **353**, 13 (1967).
6. H. G. VON SCHNERING, AND P. BLECKMAN, *Naturwissenschaften* **55**, 342 (1968).
7. J. RAVEZ AND R. DE PAPE, *Bull. Soc. Chim. Fr.*, 3283 (1966).
8. D. DUMORA AND J. RAVEZ, *C. R. Acad. Sci. Paris Ser. C* **268**, 337 (1969).
9. D. DUMORA, J. RAVEZ, AND P. HAGENMULLER, *Bull. Soc. Chim. Fr.*, 1301 (1970).
10. R. VON DER MÜHLL, D. DUMORA, J. RAVEZ, AND P. HAGENMULLER, *J. Solid State Chem.* **2**, 262 (1970).
11. J. C. COUSSEINS AND M. SAMOUEL, *C. R. Acad. Sci. Paris Ser. C* **265**, 1121 (1967).
12. J. C. COUSSEINS AND M. SAMOUEL, *C. R. Acad. Sci. Paris Ser. C* **266**, 915 (1968).
13. M. SAMOUEL AND A. DE KOZAK, *C. R. Acad. Sci. Paris Ser. C* **268**, 1789 (1969).
14. M. SAMOUEL AND A. DE KOZAK, *C. R. Acad. Sci. Paris Ser. C* **268**, 2312 (1969).
15. M. SAMOUEL, *C. R. Acad. Sci. Paris Ser. C* **270**, 1805 (1970).
16. M. SAMOUEL, *Rev. Chim. Miner.* **8**, 533 (1971).
17. E. T. KEVES, S. C. ABRAHAMS, AND J. L. BERNSTEIN, *J. Chem. Phys.* **53**, 3279 (1970).
18. J. CHENAVAS, J. J. CAPPONI, J. C. JOUBERT, AND M. MAREZIO, *Mater. Res. Bull.* **9**, 13 (1974).
19. R. D. SHANNON, *Acta Crystallogr. Sect. A* **32**, 751 (1976).
20. D. BABEL, *Z. Naturforsch. A* **20**, 165 (1965).
21. D. BABEL, *Z. Anorg. Allg. Chem.* **369**, 117 (1969).
22. H., STEINFINK AND G. BRUNTON, *Inorg. Chem.* **8**, 1665 (1969).
23. G. FERÉY, R. DE PAPE, M. POULAIN, D. GRANDJEAN, AND A. HARDY, *Acta Crystallogr. Sect. B* **33**, 1409 (1977).
24. M. SAMOUEL AND A. DE KOZAK, *Rev. Chim. Miner.* **14**, 471 (1977).
25. P. COPPENS, *Acta Crystallogr.* **18**, 1035 (1965).
26. J. Y. LE MAROUILLE, Thèse de 3ème cycle, Rennes (1972).
27. C. T. PREWITT, "SFLS-5: A Fortran IV Full Matrix Crystallographic Least Squares Program" (1966).
28. D. F. GRANT, R. C. G. KILLEAN, AND J. L. LAWRENCE, *Acta Crystallogr. Sect. B* **25**, 374 (1969).
29. V. VAND, P. F. EILAND, AND R. PEPINSKY, *Acta Crystallogr.* **10**, 303 (1957).
30. J. B. FORSYTH AND M. WELLS, *Acta Crystallogr.* **12**, 412 (1959).
31. F. H. MOORE, *Acta Crystallogr.* **16**, 1169 (1963).
32. "International Tables for X-Ray Crystallography," Vol. IV, Kynoch Press, Birmingham (1968).